The Formin INF2 Regulates Basolateral-to-Apical Transcytosis and Lumen Formation in Association with Cdc42 and MAL2

Ricardo Madrid,[1,*] Juan F. Aranda,[1] Alejo E. Rodríguez-Fraticelli,[1] Leandro Ventimiglia,[1] Laura Andrés-Delgado,[1]
Mona Shehata,[2] Susan Fanayan,[2] Hamideh Shahheydari,[2] Sergio Gómez,[1] Alberto Jiménez,[1]
Fernando Martín-Belmonte,[1] Jennifer A. Byrne,[2] and Miguel A. Alonso[1,*]
[1]Centro de Biología Molecular Severo Ochoa, CSIC/UAM, Cantoblanco, 28049 Madrid, Spain
[2]Oncology Research Unit and the University of Sydney Department of Pediatrics and Child's Health, The Children's Hospital at Westmead, Westmead, NSW 2145, Australia
*Correspondence: ricardo-m@cbm.uam.es (R.M.), maalonso@cbm.uam.es (M.A.A.)
DOI 10.1016/j.devcel.2010.04.001

SUMMARY

Transcytosis is a widespread pathway for apical targeting in epithelial cells. MAL2, an essential protein of the machinery for apical transcytosis, functions by shuttling in vesicular carriers between the apical zone and the cell periphery. We have identified INF2, an atypical formin with actin polymerization and depolymerization activities, which is a binding partner of MAL2. MAL2-positive vesicular carriers associate with short actin filaments during transcytosis in a process requiring INF2. INF2 binds Cdc42 in a GTP-loaded-dependent manner. Cdc42 and INF2 regulate MAL2 dynamics and are necessary for apical transcytosis and the formation of lateral lumens in hepatoma HepG2 cells. INF2 and MAL2 are also essential for the formation of the central lumen in organotypic cultures of epithelial MDCK cells. Our results reveal a functional mechanism whereby Cdc42, INF2, and MAL2 are sequentially ordered in a pathway dedicated to the regulation of transcytosis and lumen formation.

INTRODUCTION

Epithelial cells organize into spherical or tubular structures with their apical surface facing a central lumen and the basolateral surface contacting adjacent cells and the extracellular matrix (Bryant and Mostov, 2008). Acquisition and maintenance of apical and basolateral polarity by epithelial cells is fundamental to the display of a central lumen. Cell polarity requires sorting of lipids and proteins and subsequent vectorial traffic to their specific surface destinations (Mellman and Nelson, 2008). Proteins destined for the apical surface travel directly from the Golgi or indirectly by making a detour to the basolateral surface before becoming internalized and transported through the cell in specialized endosome carriers in a process known as transcytosis. Apical transport in epithelial cells relies on the use of these direct and indirect pathways to different degrees, depending on the type of tissue (Rodriguez-Boulan et al., 2005).

Hepatocytes are specialized epithelial cells that delimit a lumen structured into tiny channels, the bile canaliculi, which is used for bile drainage. Unlike columnar epithelial cells, whose luminal domain is located at the cell's apex and forms a central lumen, the luminal domain of hepatocytes is present in the lateral surface and delimits a bile canaliculus. Lumen positioning is regulated by Par1, which regulates the organization of the microtubule network (Cohen et al., 2004). MAL2 is an integral membrane protein originally identified in a yeast two-hybrid screen by its interaction with tumor protein D52 (Wilson et al., 2001), the founder member of a family of proteins frequently overexpressed in breast carcinoma (Boutros et al., 2004). MAL2 has proved to be an essential element of the machinery for basolateral-to-apical transcytosis in the HepG2 cell line (de Marco et al., 2002), a model of the hepatic cell. At steady state, MAL2 predominantly distributes in a Rab11^{+} subapical endosome compartment in both HepG2 cells (de Marco et al., 2002, 2006) and epithelial cells (Marazuela et al., 2004). Soon after basolateral endocytosis of apical cargo, a fraction of MAL2 redistributes from the apical region into peripheral endosome elements to concentrate internalized cargo. These endosomes then progressively fuse and move toward the apical surface for cargo delivery (de Marco et al., 2006).

Formins are a widely expressed family of proteins that nucleate the formation of actin filaments. Unlike the actin-related protein 2/3 (Arp2/3) complex, which generates branched filaments, formins form linear filaments (Ridley, 2006). The best-studied formins are the diaphanous-related formins (Drfs), which are direct effectors of Rho-family GTPases (Goode and Eck, 2007). Drfs have at their carboxyl terminus an autoregulatory domain, known as the diaphanous autoregulatory domain (DAD), which is separated by formin homology (FH) domains 1-2 from an amino-terminal diaphanous inhibitory domain (DID). The DAD interacts with the DID to close the Drf molecule and maintains it in an inactive state. The binding of the effector Rho GTPase regulates Drf activity by opening up the Drf molecule (Otomo et al., 2005). Drfs have been found to modulate a number of intracellular processes, such as endosome motility, microtubule stabilization, and cytokinesis (Faix and Grosse, 2006).

To obtain insights into the mechanism of transcytosis, we have sought proteins that interact with MAL2 and have identified human *in*verted *f*ormin (INF) 2, a formin organized in DID, FH1-2, and DAD domains, which has the unique ability to accelerate both actin polymerization and depolymerization (Chhabra and Higgs, 2006). The results presented in this work indicate the existence of a novel pathway by which Cdc42 controls apical transcytosis and correct lumen formation by regulating MAL2 dynamics through INF2.

RESULTS

Identification of Human INF2 as a MAL2-Interacting Formin

A yeast two-hybrid screen of a breast carcinoma cDNA expression library was performed with a full-length MAL2 bait (Fanayan et al., 2009). One of the cDNAs isolated, named 255C1, corresponds to a partial cDNA encoding the 255 carboxy-terminal amino acids of the human INF2-1 formin (see Figures S1A and S1B available online). Human INF2-1 consists of a 1249 residue sequence (Figure S1B) organized into DID, FH1-2, DAD, and a carboxy-terminal (C) domain, as described for mouse INF2-1 (Chhabra and Higgs, 2006). The 255C1 INF2-1 prey reproducibly bound full-length MAL2 and deleted MAL2 baits lacking the N-terminal domain (MAL2ΔN) or the N-terminal and the first membrane-associated domains (MAL2ΔNTM1), but did not detectably bind a deleted MAL2 bait additionally lacking the second membrane-associated domain (MAL2ΔNTM12) (Figure 1A). These results indicate that MAL2 residues S56–F86 that include the second hydrophobic segment are required for INF2-1 binding in this assay. In addition to INF2-1, whose C domain ends with a CIVQ sequence that in mouse INF2-1 is farnesylated (Chhabra et al., 2009), a second *INF2* cDNA was found to encode an isoform, INF2-2, in which the last 18 amino acid sequence of the INF2-1 carboxyl terminus was substituted by a 9 amino acid sequence containing basic amino acids (Figures S1A and S1B). The primary structure of human INF2-1 is 73% identical to that of mouse INF2-1 (Figure S1C). The greatest differences occur within the FH1 domain, which is shorter in human INF2, and in the C domain. Phylogenetic analysis indicated that INF2 is more closely related to Drfs Dia 1–3 than to other formins (Figure S1D). Northern blot analysis of different human tissues suggested that INF2 mRNA is ubiquitously expressed (Figure S1E). The antibodies generated to two INF2 peptides detected endogenous INF2 in a panel of human cell lines and in Madin-Darby canine kidney (MDCK) cells (Figures S1F–S1H).

Consistent with the results of yeast two-hybrid experiments, MAL2 bound to an INF2-1 fragment containing most of the C domain in pull-down experiments using a GST fusion (Figure 1B). A similar result was obtained with the similar fragment of INF2-2. The FH2DAD fragment, which contains the initial amino acids of the C domain, also bound MAL2, although it did so to a lesser extent than did the GST-C fusions. Coimmunoprecipitation experiments confirmed the association of INF2 and MAL2 (Figure 1C).

HepG2 cells polarize in vitro with their apical surface, forming intercellular lumens reminiscent of bona fide bile canaliculi (Sormunen et al., 1993). The fact that polarized apical trafficking in hepatic cells is simpler than in other model cell lines (Bastaki et al., 2002) led us to choose HepG2 cells for the functional study of INF2. A small fraction of endogenous INF2 colocalized with MAL2 at the apical membrane of HepG2 cells, whereas the remaining INF2 distributed throughout the cytoplasm (Figure 1D). Exogenous INF2-1 and INF2-2 reproduced the presence of endogenous INF2 at the apical membrane (Figure 1E), INF2-1 being mostly distributed in the endoplasmic reticulum, as described for mouse INF2-1 (Chhabra et al., 2009). Although a high level of colocalization between INF2 and calnexin was observed at the endoplasmic reticulum, calnexin was nearly depleted at the canalicular zone whereas INF2 was still present (Figures S1I and S1J). In keeping with its interaction with MAL2, the C domain of INF2-1 and INF2-2 continued to target to the apical region, as observed for the entire molecule (Figure 1F). Therefore, the C domain is the main determinant of the interaction of INF2 with MAL2 and the targeting of INF2 to the apical zone.

INF2 Silencing Impairs Lumen Formation, MAL2 Targeting to the Apical Surface, and Basolateral-to-Apical Transcytosis

To investigate the possible role of INF2 in MAL2 localization and function, we used a loss-of-function strategy by employing specific siRNA1 (si1) or siRNA2 (si2) targeted to the 3′ untranslated or coding regions of human *INF2* mRNA, respectively. Expression of si1 or si2 reduced the levels of endogenous INF2 to approximately 7% or 15%, respectively, of the INF2 content of control siRNA (siC)-transfected cells (Figures 2A and 2B). INF2 silencing greatly diminished the number of intercellular lumens (Figure 2C), decreased the size of the remaining lumens (Figure 2D), and caused a reduction in the levels of MAL2 at the apical zone in these lumens (Figures 2E and 2F). The loss of MAL2 from the apical zone was compensated for by its increased presence in scattered vesicular structures (Figure 2F).

MAL2 was previously shown to be essential for efficient transcytosis to the apical surface of both the polymeric immunoglobulin receptor and CD59, which are attached to the membrane by a single anchor, a transmembrane span or a glycosylphosphatidylinositol moiety, respectively (de Marco et al., 2002). As INF2 depletion affects the apical distribution of MAL2, we investigated whether transcytosis takes place in the absence of INF2 expression by analyzing the transport of CD59 to the luminal surface. Whereas approximately 75% of the intercellular lumens were scored as positive for transcytosed CD59 in siC-treated cells after 90 min of transcytosis, the percentage dropped to 35%–40% in the remaining lumens of INF2-silenced cells (Figure 2G; Figure S2A). Moreover, the levels of transcytosed CD59 were greatly diminished in INF2-silenced cells even in the lumens scored as positive for CD59 transcytosis (Figure 2H). The internalized CD59 in INF2-depleted cells accumulated in endosome structures distant from the apical membrane (Figure S2B), similar to the pattern observed in MAL2-silenced cells (de Marco et al., 2002). The number and size of the lumens, the levels of apical MAL2, and the access of CD59 to the apical membrane were closely associated with INF2 expression, as confirmed in HepG2 cells expressing intact INF2-2 proteins designed to be resistant (HepG/R1 cells) or sensitive (HepG/S1 cells) to expression of si1 but sensitive to si2 expression (Figure 2; Figure S2C).
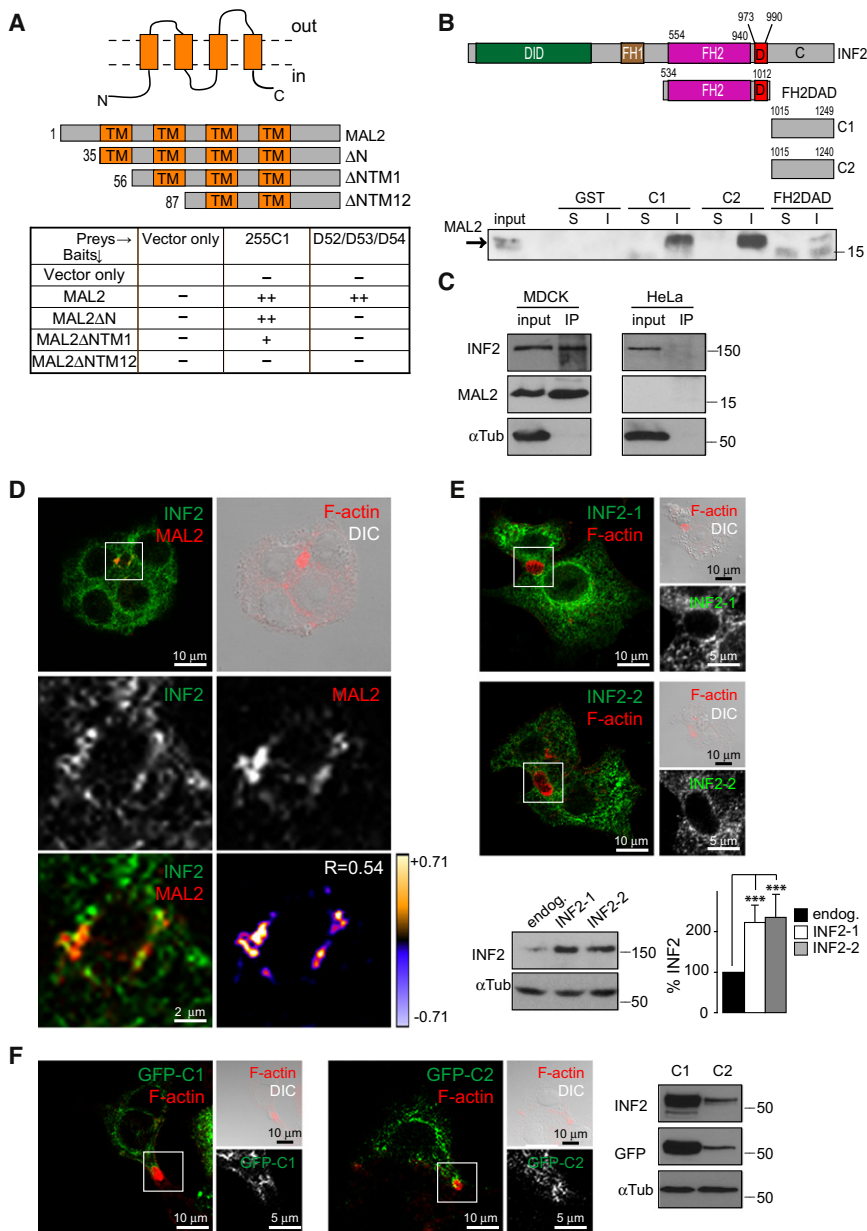
Figure 1. Characterization of INF2 as a MAL2-Interacting Protein and Analysis of Its Subcellular Distribution

(A) Yeast HF7C strain cells were cotransformed with the pAD-GAL4 255C1 cDNA obtained in the yeast two-hybrid screen and bait constructs encoding either full-length MAL2 or the indicated MAL2 proteins. Yeast growth on solid media at 30°C was evaluated as follows: –, no growth after 6–8 days; + or ++, growth after 5-6 or 3-4 days, respectively. Interactions between full-length MAL2 and D52-like prey proteins were employed as controls. Identical results were obtained for all three D52-like (D52, D53, and D54) baits, which were grouped together in a single column. A schematic of the predicted structure of MAL2 is shown.

(B) MAL2-enriched (I) or -depleted (S) membrane fractions obtained from HepG2 cells were subjected to pull-down analysis with GST fusions of the C domain of INF2-1 (C1) or of INF2-2 (C2) or the FH2DAD fragment of INF2. The presence of MAL2 was determined by immunoblotting.

(C) An MDCK cell lysate was immunoprecipitated with anti-MAL2 antibodies and the immunoprecipitates were immunoblotted with antibodies to INF2, MAL2, or α-tubulin. HeLa cells, which express INF2 but not MAL2, were used as a control of the immunoprecipitation procedure.

(D) HepG2 cells were stained for endogenous INF2, MAL2, and F-actin. An image reconstructed from different confocal planes is shown (top left panel). The position of the lumen is indicated by the boxed region. The enlargement of the boxed region shows the individual distribution of INF2 and MAL2 at the apical zone in a single x-y plane (middle panels) and the merged image (bottom left panel). Pixels where INF2 and MAL2 colocalize are depicted in a false-color image obtained by intensity correlation analysis (bottom right panel). The numbers on the false-color scale are intensity correlation coefficients. R indicates Mander's colocalization value for MAL2 and INF2 at the apical zone.

(E and F) HepG2 cells stably expressing Myc-tagged forms of INF2-1 or INF2-2 (E) or transiently expressing GFP fusions of the C domain of INF2-1 or INF2-2 (F) were used to analyze the distribution of exogenous INF2 proteins and F-actin. A representative image reconstructed from different confocal planes (E) or a single confocal x-y plane (F) is shown in the left panels. An enlargement of the apical zone from a single equatorial x-y plane (boxed region) is shown on the right of each panel. A Nomarsky image of the cell field is also included. The expression levels of INF2-1 and INF2-2 (E) and those of C1 and C2 (F) were analyzed by immunoblotting. The histogram in (E) shows the percentage of INF2-1 and INF-2 expression relative to endogenous (endog.) INF2. The mean ± SEM from three independent experiments is shown (***p < 0.001). See also Figure S1.

The exogenous expression of mDia1 (Figure S2D) was unable to correct the defects observed in lumen formation in INF2-silenced cells (Figure 2C), confirming the specific requirement of INF2. These results indicate that INF2 is required for lumen formation and efficient transcytosis to the apical membrane of HepG2 cells.

INF2 Silencing Impairs the Translocation of Apical MAL2 to Encounter Internalized Cargo

MAL2 mediates transcytosis by emitting vesicles and tubular extensions from the apical region to encounter internalized cargo dispersed at the basolateral periphery (de Marco et al., 2006). To investigate whether INF2 is required for MAL2 redistribution, we compared the dynamics of MAL2 in normal and INF2-silenced cells during CD59 transcytosis in HepG2 cells stably expressing GFP-MAL2 (HepG2/GFP-MAL2). MAL2 was initially detected solely in the luminal area in normal and INF2-silenced cells but, whereas emission of MAL2 tubules and vesicles to the cell interior took place by maturation of buds, in INF2-silenced cells buds formed but did not detach efficiently (Figures 3A and 3B; Movie S1). Different endosome profiles labeled for MAL2, F-actin, and internalized CD59 or endogenous INF2 were
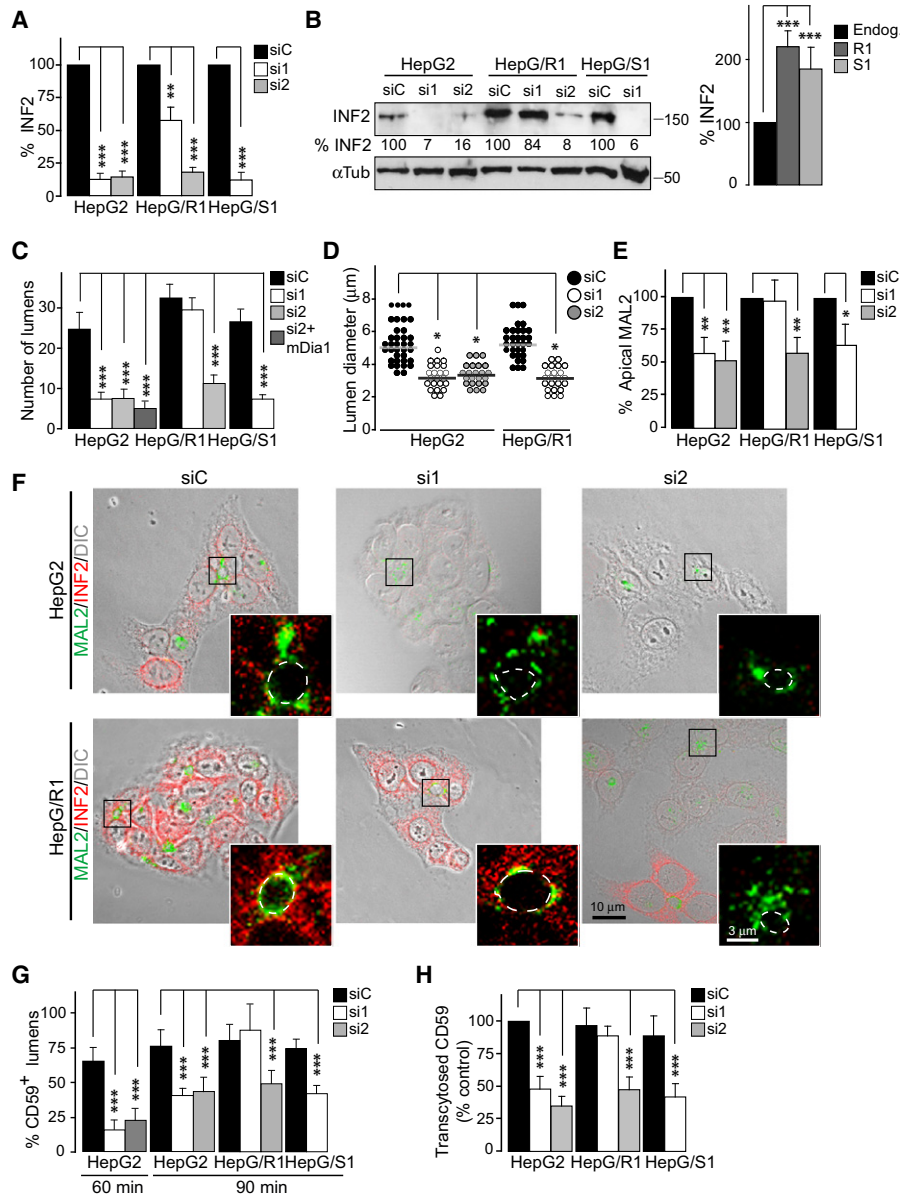
Figure 2. INF2 Silencing Decreases the Apical Levels of MAL2 and Apical Transcytosis

The three types of HepG2 cells were transfected with the indicated siRNA for 72 hr and subjected to different processing.

(A) Cells were processed for immunofluorescence labeling of INF2. The intensity of the staining was measured in >50 cells per experiment. The histogram represents the percentage of the INF2 signal relative to the corresponding siC-transfected cell.

(B) Cells were lysed and subjected to immunoblotting with anti-INF2 or anti-α-tubulin antibodies. The numbers under the INF2 blot indicate the percentage of INF2 levels, as measured by densitometric analysis, relative to the corresponding siC-transfected cell. The histogram on the right represents the total levels of INF2 in HepG/R1 and HepG/S1 cells expressed as the percentage relative to the INF2 content in siC-treated HepG2 cells.

(C) The number of intercellular lumens in the different cell cultures was quantified by analyzing 100 cells per experiment. A control with normal HepG2 cells expressing si2 for 72 hr and then expressing exogenous mDia1 for 24 hr is included.

(D) The diameter of the lumen in the different cell cultures was determined by analyzing at least 100 cells per assay. The result of a representative experiment and the mean from three independent experiments are shown.

(E) The fluorescence intensity of MAL2 at the apical region was quantified in >25 lumens in each type of cell per experiment. The result is expressed as the percentage fluorescence intensity of apical MAL2 relative to that in siC-transfected cells.

(F) A representative example of the overall distribution of MAL2 under the different conditions. A single confocal x-y plane is shown. Enlarged details of the staining at the luminal zone within the boxed regions are shown. INF2 staining was done in parallel. The contour of the lumens, obtained from phase-contrast images, is indicated by dotted lines. This experiment was done in parallel with the silencing analysis shown in (B).

(G and H) The number of lumens scored as positive for transcytosed CD59 after 60 or 90 min of transcytosis (G) and the intensity of CD59 staining in the positive lumens were determined (H). At least 50 lumens were analyzed in each case. Data are expressed as the percentage of CD59-positive lumens (G) or the levels of transcytosed CD59 expressed as the percentage relative to those in siC-transfected normal HepG2 cells (H).

Data in (A)–(E), (G), and (H) are summarized as means ± SEM from three independent experiments (*p < 0.05; **p < 0.01; ***p < 0.001). See also Figure S2.
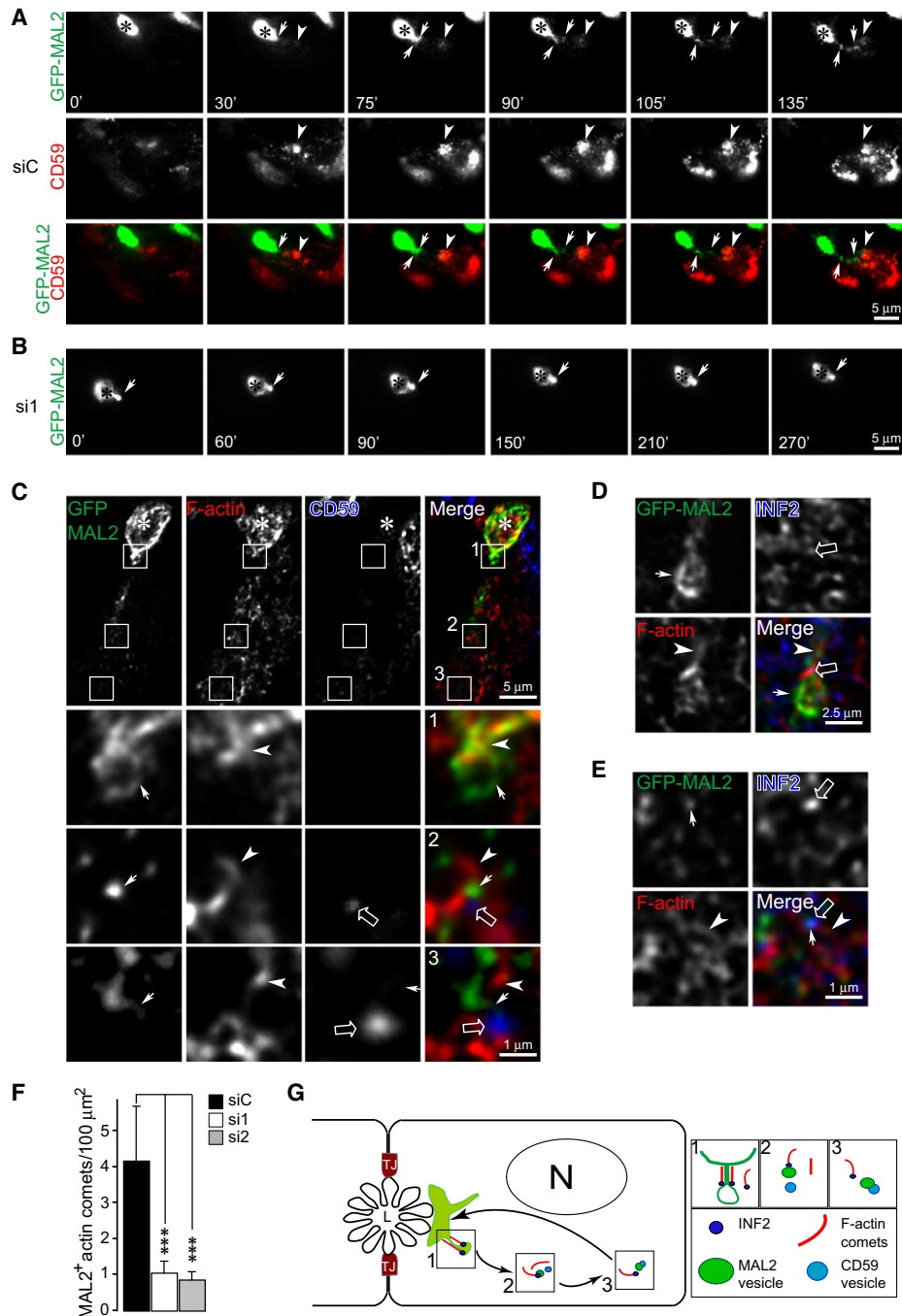
Figure 3. INF2 Silencing Impairs the Redistribution of Apical MAL2 to Meet Cargo for Apical Transcytosis

(A and B) HepG2/GFP-MAL2 cells with either normal (A) or silenced levels (B) of INF2 were sequentially incubated with anti-CD59 and fluorescent anti-mouse IgG antibodies at 4°C, washed, and incubated at 37°C to allow transcytosis of CD59. After 10 min, cells underwent time-lapse videomicroscopy to detect MAL2 and CD59 (A) or MAL2 (B). Selected sequential frames from a representative experiment are shown. The asterisks indicate the position of the lumen. The arrows point to MAL2-positive buds and elements that arise from the apical region, and the arrowheads indicate MAL2-positive structures emitted from the luminal zone that are positive for internalized CD59. See also Movie S1.

(C–E) Still images obtained by confocal microscopy of different events occurring early during transcytosis. The enlargements show details of the boxed regions indicating the positions of MAL2 (filled arrow), actin filaments (arrowhead), and internalized CD59 (open arrow) (C) or INF2 (open arrow) (D and E) after 20 min of transcytosis. The asterisks in (C) indicate the position of the lumen. A single confocal x-y plane is shown.

(F) The number of cytoplasmic MAL2-positive elements with associated actin comets was quantified and represented as mean ± SEM. Three independent experiments were performed (***$p < 0.001$).

(G) Schematic representation of different events visualized during transcytosis. A MAL2-positive bud detaching from the apical region (box 1) and a MAL2-positive vesicle approaching (box 2) or fusing (box 3) with an endosome vesicle containing basolaterally internalized CD59.

captured early during CD59 transcytosis. Figure 3C shows a MAL2-positive bud arising from the apical zone that is surrounded by F-actin at the site of bud attachment (box 1), a MAL2-positive element with a short actin comet encountering a vesicle loaded with internalized CD59 in the middle of the cell (box 2), and a MAL2-positive profile emitting extensions to contact a vesicle with internalized CD59 at the cell periphery (box 3). Figures 3D and 3E show a MAL2-positive apical bud associated with INF2 and F-actin and a peripheral MAL2-positive transport vesicle with INF2 and an associated actin comet, respectively. It is of particular note that silencing of INF2 greatly reduced the number of cytoplasmic MAL2-positive vesicular elements associated with actin comets (Figure 3F). Therefore, INF2 is required for the formation of actin comets that allow the emission of MAL2-positive elements from the apical membrane and their movement to encounter basolaterally internalized cargo (Figure 3G).

INF2 Function in Transcytosis Is Lost by Mutation of Critical Residues Involved in Actin Polymerization or Depolymerization

Mutation of three critical leucine residues (Leu1010, Leu1011, Leu1020) to alanine in the DAD of mouse INF2 abrogates the in vitro depolymerization but not the polymerization activity of INF2 (Chhabra and Higgs, 2006). Substitution of Lys1601 in the FH2 domain of yeast formin Bni1p and of the corresponding lysine residue of mDia2 (Lys853) by alanine abolishes the actin nucleation activity of these formins (Bartolini et al., 2008; Xu et al., 2004). As all these residues are conserved in human INF2 (Figure 4A), we introduced the same replacements at the equivalent positions of human INF2-2 (Lys792 and Leu976, Leu977 and Leu986) to express INF2 proteins (INF2-K/A and INF2-3L/A) with these mutations. As transient overexpression of INF2-3L/A was toxic to the cells, we prepared stable transfectants, whereas in the case of INF2-K/A we used transient expression. We then examined whether INF2-3L/A or INF2-K/A, which were designed to resist si1 but not si2 expression, as actually occurred (Figure 4A), can functionally replace endogenous INF2 in si1-transfected cells as intact INF2-2 did (Figure 2). The stable expression of INF2-3L/A produced a 40% reduction in the number of intercellular lumens relative to normal HepG2 cells (Figure 4B). Silencing the endogenous protein alone with si1 in HepG2 INF2-3L/A cells caused an additional 20% decrease, and knockdown of both the endogenous and the exogenous protein with si2 produced a further 8% drop (Figure 4B). The failure of INF2-3L/A to replace endogenous INF2 in lumen formation parallels its ineffectiveness in mediating CD59 transcytosis (Figures 4C–4E) and is correlated with a significant reduction in the number of cytoplasmic MAL2-positive vesicles associated with actin comets (Figure 4F). Similarly, the INF2-K/A mutant was also unable to replace endogenous INF2 in lumen formation, apical transcytosis, and association of actin comets to MAL2-positive vesicles, although the effects of INF2-K/A were milder than those of the INF2-3L/A mutant (Figures 4B–4F). Thus, INF2 requires its actin depolymerization activity and an intact FH2 domain to mediate normal lumen formation and efficient transcytosis in HepG2 cells.

Next, we carried out gain-of-function experiments by expressing ΔDID and ΔDIDΔC INF2-2 proteins lacking the DID domain,

which is required for closing Drfs in an inactive state. Expression of both mutants in HepG2 cells (Figure 4G) induced formation of long longitudinal actin stress fibers (Figure S3A), alignment of microtubules along the actin fibers (Figure S3A), cell depolarization (Figure S3B), and development of long filopodial structures (Figures 4H–4J; Figures S3A–S3C). Filopodia induced by the mutants were often long, up to 6–8 μm (Figure 4H), and were not attached to the substratum, resembling those induced by an mDia2 mutant with a similar N-terminal deletion (Yang et al., 2007). Cell depolarization and formation of long filopodia were also induced by the two INF2-2 deletion mutants in MDCK cells (Figures S3D–S3G). Both mutants were detected at the tip of most of the filopodium processes present in transfected HepG2 cells (Figure 4I, left histogram; Figure 4J). It is of particular note that the distribution of MAL2 in these cells was affected differently by the mutants. ΔDID INF2-2, which keeps the MAL2-interacting C region intact, induced the recruitment of MAL2 to the F-actin tips at the cell edges, where MAL2 and the ΔDID mutant colocalized, whereas ΔDIDΔC INF2-2, which lacks the MAL2-interacting C region, did not target MAL2 to the F-actin tips (Figure 4I, right histogram; Figure 4J). As a control, we observed that expression of intact INF2-2 did not alter the perinuclear MAL2 distribution found in the unpolarized population of HepG2 cells (Figure 4J). The results in Figures 4H–4J provide an extreme case showing that the intracellular distribution of MAL2 is governed by INF2 through the formation of actin filaments and its physical interaction with MAL2.

Cdc42 Binds INF2 and Regulates Lumen Formation, MAL2 Dynamics, and Apical Transcytosis

To investigate the binding of Rho GTPases to the DID of INF2, we performed pull-down assays (Figure 5A). Cdc42 bound to the INF2 fragment exclusively in its GTP-loaded form, whereas Rac1 binding occurred regardless of its state of loading, although to different extents. No binding of RhoA was observed in either case, consistent with the fact that INF2 lacks an extension N-terminal to the DID (Chhabra et al., 2009) that is present in the RhoA-regulated Drfs mDia1-2 and that in mDia1 is involved in RhoA binding (Otomo et al., 2005). The silencing of Cdc42 basically reproduced the effects of INF2 silencing with regard to the number of lumens, the percentage of remaining lumens with transcytosed CD59, and the levels of transcytosed CD59 in these lumens (Figures 5B–5F). In contrast, RhoA and Rac1 silencing did not affect the number of lumens or the percentage of lumens with transcytosed CD59 (Figures 5B–5F) and produced only mild effects on the luminal levels of transcytosed CD59 (Figure 5E). Therefore, Cdc42 appears to be the Rho-GTPase regulator of INF2 for the processes of lumen formation and apical transcytosis, although we cannot rule out a role for Rac1 as an INF2 regulator in other cellular processes.

It is of particular note that a fraction of active Cdc42 mutant (Cdc42L61) was distributed at the apical membrane where it colocalized with MAL2, the remainder being distributed throughout the cytosol (Figure 6A). In accordance with the results from Cdc42-silenced cells, overexpression of a dominant-negative form of Cdc42 (Cdc42N17) in HepG2 cells dramatically reduced the number of lumens, whereas the active mutant had the opposite effect (Figure 6B). Moreover, Cdc42L61 accelerated CD59 transcytosis in such a way that,
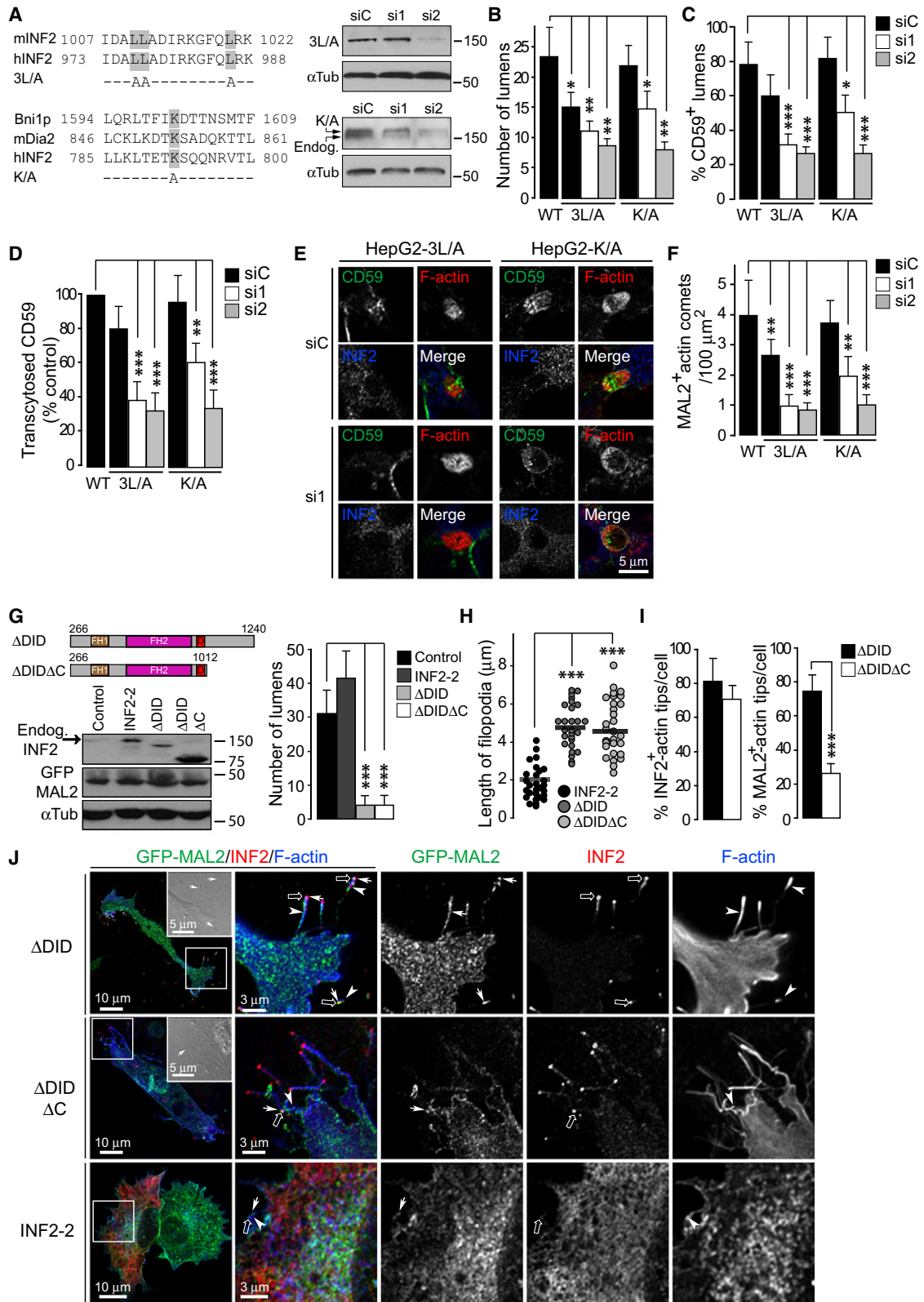
Figure 4. Effect of Expression of INF2 Proteins with Point Mutations or Domain Deletions in HepG2 Cells

(A) The alignments show the DAD sequence of human and mouse INF2 (top left panel) and the conservation of Lys1601 in the FH2 domain of Bni1p in the corresponding position of mDia2 and human INF2 (bottom left panel). The residues mutated to alanine in the 3L/A and K/A INF2-2 mutants are indicated.

after 30 min at 37°C, approximately 42% of the lumens formed already contained transcytosed CD59, in contrast to only 7% in the GFP-transfected control (Figure 6C). Importantly, the increased rate of transcytosis promoted by Cdc42L61 was accompanied by increased dynamics of MAL2, as revealed by experiments in which the recovery of apical GFP-MAL2 fluorescence at the expense of the cytoplasmic pool was measured (Figure 6D). Providing further evidence of a role for Cdc42 and INF2 in the regulation of MAL2 function in transcytosis, MAL2 dynamics in normal cells were reduced by Cdc42 or INF2 silencing (Figure 6D). Moreover, consistent with a role of INF2 and MAL2 downstream of Cdc42, silencing of INF2 or MAL2 (Figure 6E) greatly decreased the number of lumens and the enhanced rate of transcytosis observed in Cdc42L61-expressing cells (Figures 6F and 6G). The knockdown of either INF2 or MAL2 caused a modest decrease in the levels of endogenous GTP-loaded Cdc42 but not in the total levels of the protein (Figure 6H). This effect is probably due to the existence of autoregulatory feedback loops between cell polarization and Cdc42 activity as described in MDCK cells (Martin-Belmonte et al., 2007). It is of note that the effect of MAL2 or INF2 depletion on lumen formation and apical transcytosis is not due to the observed reduction in Cdc42 activity, as the expression of active Cdc42L61 in cells knocked down for MAL2 or INF2 did not correct the defects (Figures 6F and 6G). Therefore, the conclusion from Figures 5 and 6 is that Cdc42 regulates apical transcytosis in HepG2 cells by controlling MAL2 dynamics through INF2 (Figure 6I).

Given the role of INF2 and MAL2 in transcytosis and lumen formation in HepG2 cells, we investigated the involvement of these two proteins in the formation of the central lumen in MDCK cells. MAL2 colocalized with an apical pool of Cdc42 in cysts of MDCK cells (Figure 7A). Silencing of endogenous MAL2 (Figure 7B) greatly inhibited the formation of central lumens in normal MDCK cells (Figures 7C and 7D) and, instead, multiple intercellular and intracellular lumens appeared (Figure 7D). Normal formation of central lumens was observed in MDCK cells stably expressing human MAL2, which is insensitive to the siRNA used to deplete the endogenous canine protein

(Figures 7B–7D). INF2 silencing in MDCK cells (Figure 7E) basically reproduced the effect of MAL2 silencing, with a dramatic drop in the formation of central lumens and the appearance of multiple inter- and intracellular lumens (Figures 7F and 7G). Thus, both INF2 and MAL2 are required for the formation of the central lumen in MDCK cell cysts.

DISCUSSION

The integral membrane MAL2 protein was characterized as an essential component of the vesicular machinery for apical transcytosis (de Marco et al., 2002). In an attempt to understand how transcytotic vesicular traffic is regulated, we sought MAL2-interacting proteins and found INF2, a formin of unknown function (Chhabra and Higgs, 2006) that is a binding partner of MAL2. The interaction involved the carboxy-terminal (C) region of INF2, which is not conserved in other formins. At the opposite end of the molecule, the DID of INF2 interacted with Cdc42 and Rac1 but not RhoA. Consistent with their physical interaction, MAL2 colocalized with a fraction of Cdc42 and INF2 at the apical region of HepG2 cells. A combination of loss- and gain-of-function experiments revealed a novel pathway by which Cdc42 binds to INF2, which, in turn, regulates MAL2 dynamics and, thereby, transcytotic transport to the apical membrane. The functioning of this pathway is essential for correct lumen formation in HepG2 cells and organotypic cultures of MDCK cells.

MAL2 fulfils its transcytotic function by shuttling in tubulovesicular structures between the apical zone, which constitutes its main site of residence, and the cell periphery, where it encounters internalized cargo that is subsequently ferried in MAL2-positive transcytotic carriers destined for the apical surface (de Marco et al., 2006). In the case of the apical MUC1 cargo glycoprotein, a direct interaction with MAL2 has recently been described (Fanayan et al., 2009). We observed that silencing of either Cdc42 or INF2 in HepG2 cells slowed down MAL2 dynamics and greatly diminished the progression of cargo toward the apical membrane without affecting its internalization. Glycosylphosphatidylinositol-anchored protein internalization

Effect of si1 and si2 transfection on INF2 levels in HepG2 cells expressing INF2-3L/A (top right panel) and INF2-K/A (bottom right panel) in stable and transient transfections, respectively. The expression of α-tubulin was taken as a loading control.

(B) The number of intercellular lumens in the different cell cultures transfected with the indicated siRNA was quantified by analyzing 100 cells per experiment.

(C and D) The number of lumens positive for transcytosed CD59 after 90 min of transcytosis (C) and the intensity of CD59 in the positive lumens were determined (D). At least 50 lumens were analyzed in each case. Data are expressed as the percentage of CD59-positive lumens (C) or the levels of transcytosed CD59 relative to those in siC-transfected normal (WT) HepG2 cells (D).

(E) A representative experiment showing the distribution of F-actin, INF2, and CD59 after 90 min of CD59 transcytosis in HepG2 cells stably or transiently expressing INF2-3L/A or INF2-K/A, respectively, transfected with siC or si1. A single confocal x-y plane from the luminal zone is shown.

(F) The number of cytoplasmic MAL2-positive elements with associated actin comets was quantified.

(G–I) HepG2/GFP-MAL2 cells were transfected for 48 hr to express the indicated INF2-2 proteins. The expression levels of INF2, MAL2, and α-tubulin were analyzed by immunoblotting (G, left panel) and the effect of the exogenous INF2-2 proteins on the number of intercellular lumens was quantified in 100 cells per assay (G, right panel). The length of filopodial protrusions was determined in at least 20 filopodia per cell in a total of 25 cells examined per assay. The result of a representative experiment and the mean from three independent experiments are shown (H). The number of actin filaments with exogenous INF2 (I, left panel) or MAL2 (I, right panel) at the tip of the filopodia induced by ΔDID or ΔDIDΔC INF2-2 was quantified. Data are expressed as the mean percentage relative to the total number of filopodia examined.

(J) A representative example of the overall distribution of MAL2, INF2, and F-actin in cells expressing the indicated exogenous INF2-2 proteins. A single confocal x-y plane is shown. A region of the cell edge is boxed in each case (left panels). A Nomarsky image of the boxed region indicating the position of the filopodia structures is also included. The enlargement of the boxed regions shows details of the distribution of MAL2 (filled arrows) and INF2 (open arrows) at the tip of the filopodial protrusions, which were visualized by F-actin staining (arrowheads). In the case of intact INF2-2 transfection, only the cell on the left was transfected. The cell on the right serves, therefore, as an internal control of the normal distribution of MAL2 in the unpolarized HepG2 cell population.

Data in (B)–(D) and (F)–(I) are summarized as means ± SEM from three independent experiments (*p < 0.05; **p < 0.01; ***p < 0.001). See also Figure S3.
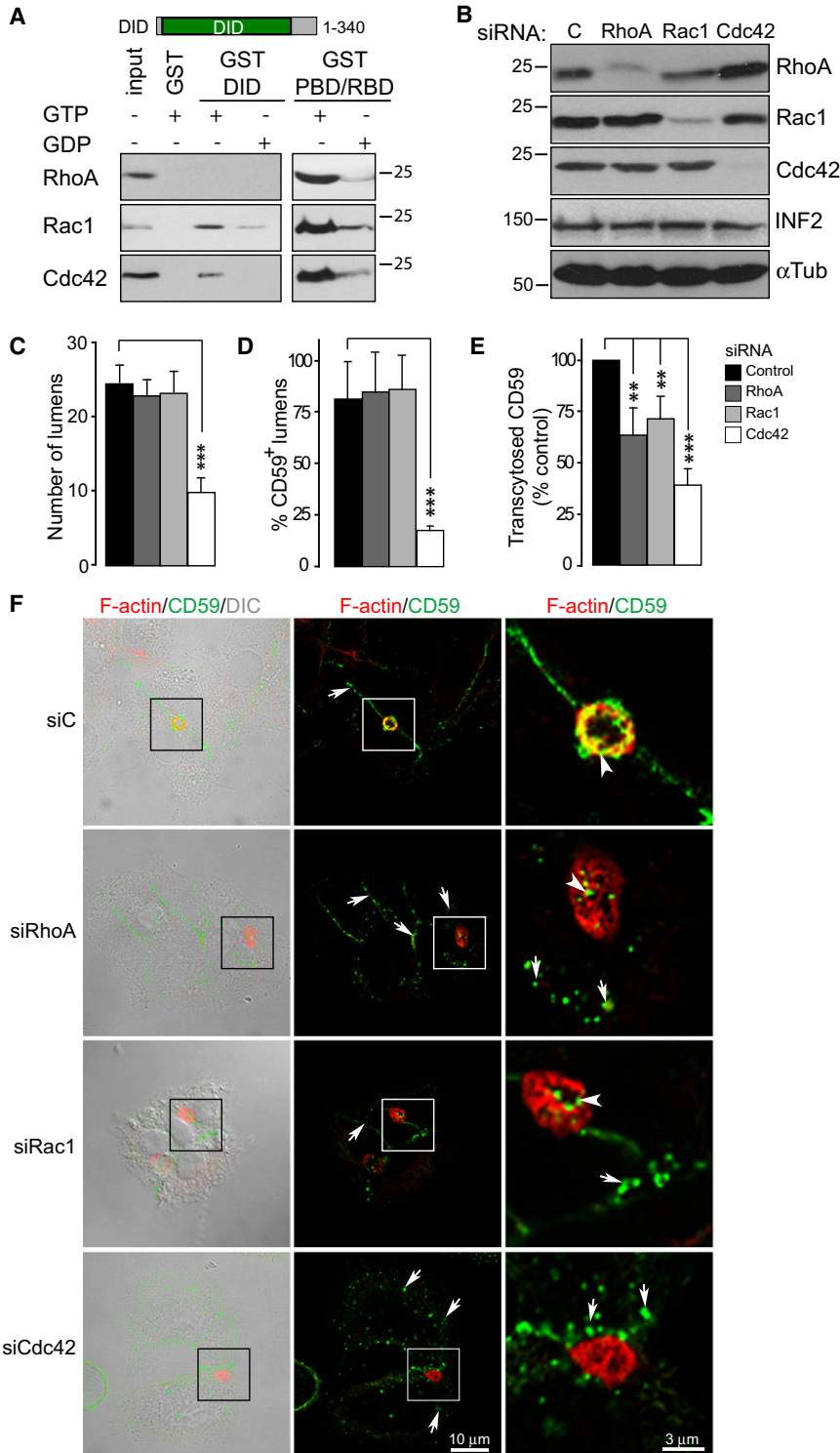
has been recently shown to be a Cdc42-independent process that requires expression of flotillin (Ait-Slimane et al., 2009), a type of raft-associated molecule structurally unrelated to MAL2. It is of particular note that INF2 silencing produced cargo retention in endosome structures distant from the apical membrane, evoking the effect of MAL2 silencing by which MAL2 appears to control transcytosis remotely (de Marco et al., 2002). Our results are in agreement with previous findings showing the requirement of actin filaments in postendocytic traffic of cargo prior to the nocodazole-sensitive step (Maples et al., 1997) and are evidence of collaboration between the actin and microtubule cytoskeletons in apical transcytosis. Although speculative at this stage, the observation that, in addition to its location at the apical zone, INF2 is predominantly localized in the endoplasmic reticulum raises the possibility of an involvement of the endoplasmic reticulum in apical transcytosis or other transport processes. Actin assembly has been shown to power
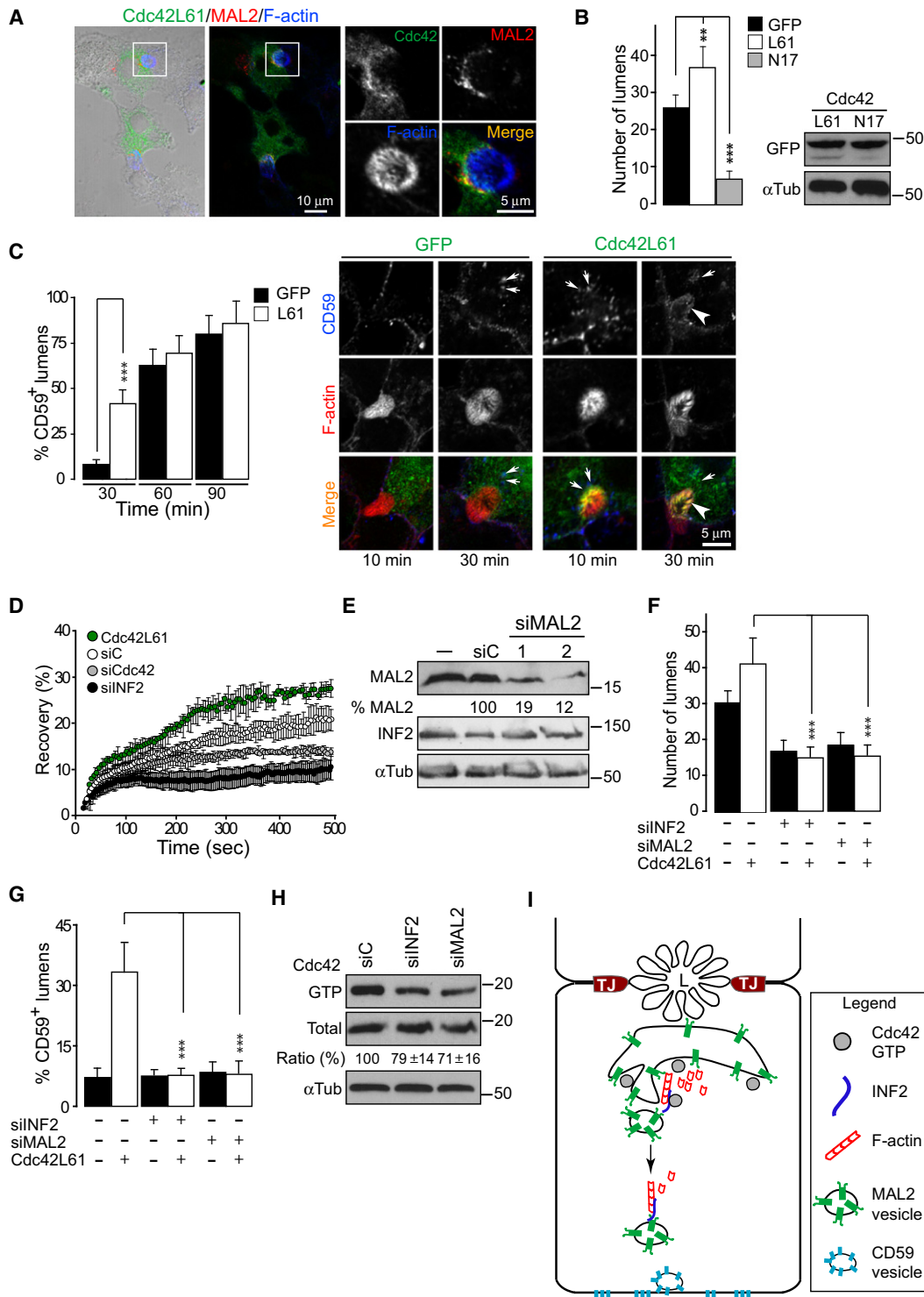
Figure 6. Cdc42 Regulates the Number of Lumens and the Rate of Transcytosis in an INF2- and MAL2-Dependent Fashion

(A) The distributions of MAL2, F-actin, and transiently expressed Cdc42L61 were analyzed by confocal microscopy. An image reconstructed from different confocal planes is shown. The position of the lumen is indicated by the boxed region (left panels). The enlargement of the boxed region shows the distribution in a single x-y plane of Cdc42, MAL2, and F-actin at the apical region (right panels).

(B and C) HepG2 cells were transfected with DNA constructs expressing GFP alone or fused to the Cdc42L61 or Cdc42N17 mutants and 24 hr later subjected to different processing. The number of intercellular lumens was quantified by analyzing 100 cells per experiment (B, left panel). The expression levels of the respective proteins were analyzed by immunoblotting (B, right panel). The number of lumens positive for transcytosed CD59 was estimated in GFP- or Cdc42L61-GFP-transfected cells after 30, 60, or 90 min of transcytosis and expressed as the percentage relative to the total number of lumens (C, left panel).

the movement of intracellular vesicles and even intracellular pathogens (Ploubidou and Way, 2001; Taunton, 2001). In vitro elongation of actin filaments between an immobilized formin and a second anchor point produces buckled filaments as short as 0.7 μm, demonstrating that actin polymerization produces forces > 1 pN (Kovar and Pollard, 2004; Kozlov and Bershadsky, 2004). We have visualized comets formed by short actin filaments decorated with INF2 at their growing end that appear to push different types of MAL2-positive elements. These actin comets were practically absent in INF2-silenced cells. It is worth noting that the expression of the deregulated ΔDID mutant, which contains the C-terminal domain responsible for the interaction of INF2 with MAL2, but not a similar mutant without this domain, resulted in MAL2 targeting to the tips of the INF2-induced actin stress fibers, where it colocalizes with the deregulated INF2 protein. We therefore propose that assembly and disassembly of short actin filaments by INF2 provide force for propelling MAL2-positive vesicle movement to encounter internalized cargo.

Formins mDia3 (hDia2C) and the couple mDia1 and mDia2 as effectors of RhoD and RhoB, respectively, show the potential to modulate endosome trafficking (Fernandez-Borja et al., 2005; Gasman et al., 2003; Wallar et al., 2007). It has been proposed that the physiological role of these Drfs is to allow endosome movement by participating in continuous polymerization-depolymerization cycles of actin filaments (Wallar et al., 2007). The formin-family Diaphanous Dia1 is required for apical secretion in epithelial tubes of the *Drosophila* embryo (Massarwa et al., 2009). Obviously, mDia1–3 would be responsible for F-actin assembly, but disassembly would require the participation of additional proteins with severing and depolymerizing activities. The participation of such proteins does not appear to be exclusive to the movement of endosomes because cofilin, an actin-severing protein, has recently been implicated in the regulation of a population of actin filaments involved in transport of p75 through the direct route from the Golgi (Salvarezza et al., 2009). A distinctive feature of INF2, compared with the aforementioned Drfs, is its in vitro capacity both to nucleate and depolymerize actin filaments (Chhabra and Higgs, 2006). Therefore, unlike other formins that would require machinery for disassembly of actin filaments, it appears that INF2 could do the entire job. Consistent with the requirement for actin assembly and disassembly in INF2 function in transcytosis, we found that INF2 proteins with mutations that abrogate the actin depolymer-

ization activity of INF2 or the actin polymerization activity of other formins were unable to reconstitute transcytosis in cells with depleted levels of endogenous INF2, whereas this was successfully achieved by intact INF2.

Unlike HepG2 cells that form lateral lumens, MDCK cells grown in three-dimensional cultures orient their apical surface to assemble a central lumen. A current model of control of epithelial morphogenesis proposes that Cdc42 is recruited to the apical surface by annexin 2, which, in turn, is recruited by PTEN-mediated apical segregation of PtdIns(4,5)P₂. Once at the apical membrane, Cdc42 can recruit Par6, a member of the Par3/Par6/aPKC complex, which controls apical membrane formation (Martin-Belmonte et al., 2007). Cdc42 silencing impairs the formation of the central lumen in MDCK cysts and, instead, multiple intracellular and intercellular lumens are formed (Martin-Belmonte et al., 2007). Silencing of INF2 or MAL2 in MDCK cells recapitulated the effect of Cdc42 silencing on lumen formation. In contrast, we did not observe formation of intracellular or intercellular lumens in HepG2 cells with silenced levels of Cdc42, INF2, or MAL2. An important difference between HepG2 and MDCK cells is that apical transport of proteins attached to the membrane by a single anchor exclusively relies on the transcytotic pathway in HepG2 cells, whereas direct routes coexist with the transcytotic pathway in MDCK cells. Therefore, in the absence of apical transcytosis, MDCK cells can still use the direct route for apical targeting and form intracellular or intercellular lumens, whereas this process is not possible in HepG2 cells.

INF2 mutations have recently been implicated in an autosomal-dominant form of focal segmental glomerulosclerosis (Brown et al., 2010), a kidney disease characterized by dysregulation of podocyte function and alterations in the podocyte cytoskeleton. As INF2 is ubiquitously expressed, our results on INF2 function could be useful for understanding the role of INF2 in other cell types under normal or pathological conditions. In summary, our findings suggest that, in addition to acting in other pathways crucial for correct lumen formation (Georgiou et al., 2008; Jaffe et al., 2008; Martin-Belmonte et al., 2007), Cdc42 governs a novel pathway dedicated to the regulation of apical transcytosis by which Cdc42 controls INF2, which, in turn, regulates MAL2 dynamics through the formation of actin comets that promote the formation of MAL2-positive elements and appear to propel their movement. This process is essential for correct lumen formation in HepG2 and MDCK cells.

The distributions of CD59 and F-actin after 10 and 30 min of transcytosis are shown (C, right panels). A single confocal x-y plane from the luminal zone is shown. The arrows and the arrowheads point to CD59 located outside the luminal zone or in the luminal membrane, respectively.

(D) HepG2/Cherry-MAL2 cells expressing siC, siINF2 (si1), or siCdc42 for 72 hr or expressing Cdc42L61 for 24 hr were assayed at different times for the recovery of apical MAL2 fluorescence after photobleaching of MAL2 at the apical area. Data are expressed as percentage recovery ± SEM from five independent experiments.

(E) HepG2 cells were transfected with siC or two different siRNAs targeted to MAL2. After 72 hr, cell extracts were analyzed with antibodies to MAL2, INF2, or α-tubulin. The levels of MAL2 expression are expressed as percentages relative to siC-transfected cells.

(F and G) HepG2 cells were transfected for 72 hr with siRNA to INF2 (si1) or to MAL2 alone or together with Cdc42L61. The number of intercellular lumens was quantified by analyzing 100 cells per experiment (F). The number of lumens positive for transcytosed CD59 was analyzed after 30 min of transcytosis and the result is expressed as the percentage relative to the total number of lumens under each condition. At least 50 lumens were analyzed in each case (G).

(H) HepG2 cells were transfected with siC or an siRNA pool targeted to INF2 or MAL2, respectively. After 72 hr, active Cdc42 was detected by pull-down assay with the GTPase binding domain of PAK followed by immunoblotting with anti-Cdc42 antibodies. Data are expressed as the mean percentage ± SEM of active Cdc42/total Cdc42 relative to siC-transfected cells.

(I) Schematic model of the proposed role of Cdc42 and INF2 in the formation and movement of MAL2-positive vesicular carriers.

Data in (B)–(D) and (F)–(H) are summarized as means ± SEM from three independent experiments (**p < 0.01; ***p < 0.001).
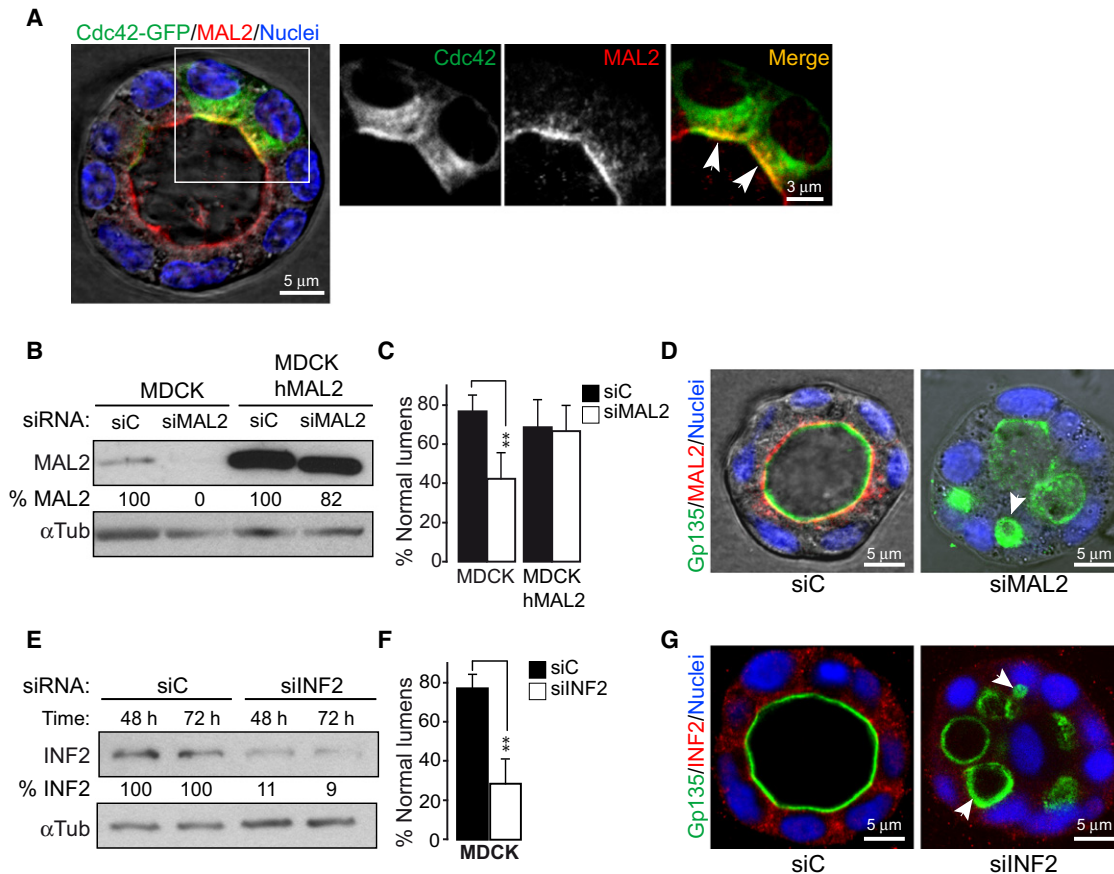
Figure 7. MAL2 and INF2 Are Necessary for Central Lumen Morphogenesis in Three-Dimensional Cultures of MDCK Cells

(A) MDCK cell cysts expressing Cdc42-GFP were grown for 72 hr and then stained for endogenous MAL2 and nuclei (left panel). The arrowheads in the enlargement of the boxed region show regions of colocalization of MAL2 with the apical pool of Cdc42 (right panels).

(B) Normal MDCK cells or MDCK cells stably expressing human MAL2 (hMAL2) were transfected with control siRNA or siRNA to canine MAL2, plated for 72 hr, and analyzed by western blot with antibodies that recognize both canine and human MAL2 or with antibodies to α-tubulin. Human MAL2 expression was not affected by the siRNA targeted to canine MAL2. The percentage of MAL2 expression under the different conditions used is indicated.

(C) Normal MDCK cells or MDCK cells stably expressing human MAL2 were transfected with control siRNA or siRNA to canine MAL2 for 24 hr and grown in Matrigel for 72 hr. Quantification of the number of cysts with normal central lumens in control MDCK cells and MDCK cells knocked down for MAL2 is shown.

(D) Normal MDCK cells treated as in (C) were fixed and stained for the apical marker Gp135, MAL2, and nuclei. MAL2-silenced cells showed impaired lumen morphogenesis and formed cysts with multiple small lumens (arrowhead).

(E) Normal MDCK cells were transfected with control siRNA or siRNA to canine INF2 for 24 hr, plated for 72 hr, and analyzed by western blot with anti-INF2 antibodies or with antibodies to α-tubulin. The percentage of INF2 expression under the different conditions used is indicated.

(F) Normal MDCK cells transfected with control siRNA or siRNA to canine INF2 for 24 hr were grown in Matrigel for 72 hr. The number of cysts with normal central lumens in control MDCK cells and MDCK cells knocked down for INF2 was quantified. Data are represented as the percentage of cysts with central lumen.

(G) Normal MDCK cells treated as in (F) were fixed and stained for the apical marker Gp135 and INF2. Cells were then fixed and stained for the apical marker Gp135, endogenous INF2, and nuclei. INF2-silenced cells showed impaired lumen morphogenesis and formed cysts with multiple small lumens (arrowheads). Data in (C) and (F) are summarized as means ± SEM from three independent experiments. More than 100 cysts were quantified in each experiment (**p < 0.01).

EXPERIMENTAL PROCEDURES

Yeast Two-Hybrid Screening

Yeast two-hybrid screening and direct interaction testing were performed as previously described (Fanayan et al., 2009). Please refer to Supplemental Information for further details of the experimental procedures used.

Cloning of Human *INF2* cDNA and Generation of *INF2* cDNA Constructs

Sequencing of several cDNAs mapping to the human *INF2* locus obtained from the IMAGE Consortium (http://image.hudsonalpha.org) allowed the identification of two overlapping halves of the human *INF2-2* cDNA coding sequence (IMAGE clones 2223558 and 3343082). These partial cDNAs were subse-

quently fused to generate a single length of cDNA of 4.6 kb, which includes the complete coding sequence of INF2-2 and a part of its 5′ and 3′ untranslated flanking regions. The rest of the DNA constructs used are described in Supplemental Information.

Cell Cultures, siRNA, and Transfections

Human hepatoma HepG2 cells were grown in high-glucose Dulbecco's modified Eagle's medium supplemented with 5% fetal bovine serum (Sigma). For stable expression of exogenous proteins, transfected cells were selected by treatment with 0.5 mg/ml G-418 sulfate for at least 4 weeks after transfection. Positive cell clones were maintained in drug-free medium. After several passages in this medium, >90% of cells retained expression of the exogenous product. To prepare cysts in Matrigel, MDCK cells grown in Petri dishes were

brought to a single-cell suspension (4×10^4 cells/ml) in 2% Matrigel, plated in coverglass chambers, and grown for 72 hr. The sequence of the siRNA heteroduplexes and the transfection conditions used are detailed in Supplemental Experimental Procedures.

Confocal Microscopic Analysis

The procedure for cell immunolabeling is detailed in Supplemental Information. Images were obtained by confocal microscopy using an LSM510 META system (Carl Zeiss) coupled to an inverted Axiovert 200 microscope. For each sample, medial optical slices of 50 different polarized cells were recorded. HepG2 intercellular lumens (bile canaliculi) were visualized on phase-contrast acquisitions and by F-actin staining. We used Huygens 3.0 software (Scientific Volume Imaging) for deconvolution and ImageJ (http://rsb.info.nih.gov/ij) for colocalization graphics. NIH Image software was used to quantify the intensity of fluorescence (mean intensity of fluorescence per pixel). Images were exported in TIFF format, and their brightness and contrast were optimized with Adobe Photoshop.

Transcytosis Assay

HepG2 cells were incubated with mouse mAb to CD59 at 4°C for 30 min. After extensive washes, cells were incubated at 37°C for different times in normal medium. At each time, the cells were washed, fixed, and analyzed by immunofluorescence microscopy with fluorescent anti-mouse IgG secondary antibodies (Invitrogen). Lumens were scored as positive for transcytosed CD59 when the intensity of CD59 staining was greater than the mean at 0 min + 1.5 × SEM.

Time-Lapse Videomicroscopic Analysis and FRAP Assays

Time-lapse videomicroscopy of the transcytosis process was as previously described (de Marco et al., 2006). Cell images were captured at 15 min intervals. Images were analyzed with MetaMorph imaging software (Molecular Devices). FRAP analysis was done with an inverted confocal laser LSM710 scanning microscope (Carl Zeiss).

Pull-Down and Coimmunoprecipitation Analyses

For pull-down experiments, HepG2 cell lysates were incubated at 4°C in assay buffer with 10 μg of GST proteins immobilized on GSH-Sepharose beads (GE Healthcare Life Sciences). For coimmunoprecipitation analysis, lysates were precleared with a control antibody bound to protein G Sepharose and then incubated overnight at 4°C with anti-MAL2 antibody complexed to protein G Sepharose. Sepharose beads were extensively washed and bound proteins were analyzed by immunoblotting. Please refer to Supplemental Information for further details.

SUPPLEMENTAL INFORMATION

Supplemental Information includes Supplemental Experimental Procedures, three figures, and one movie and can be found with this article online at doi:10.1016/j.devcel.2010.04.001.

REFERENCES

Ait-Slimane, T., Galmes, R., Trugnan, G., and Maurice, M. (2009). Basolateral internalization of GPI-anchored proteins occurs via a clathrin-independent flotillin-dependent pathway in polarized hepatic cells. Mol. Biol. Cell 20, 3792–3800.

Bartolini, F., Moseley, J.B., Schmoranzer, J., Cassimeris, L., Goode, B.L., and Gundersen, G.G. (2008). The formin mDia2 stabilizes microtubules independently of its actin nucleation activity. J. Cell Biol. 181, 523–536.

Bastaki, M., Braiterman, L.T., Johns, D.C., Chen, Y.H., and Hubbard, A.L. (2002). Absence of direct delivery for single transmembrane apical proteins or their "secretory" forms in polarized hepatic cells. Mol. Biol. Cell 13, 225–237.

Boutros, R., Fanayan, S., Shehata, M., and Byrne, J.A. (2004). The tumor protein D52 family: many pieces, many puzzles. Biochem. Biophys. Res. Commun. 325, 1115–1121.

Brown, E.J., Schlondorff, J.S., Becker, D.J., Tsukaguchi, H., Uscinski, A.L., Higgs, H.N., Henderson, J.M., and Pollak, M.R. (2010). Mutations in the formin gene INF2 cause focal segmental glomerulosclerosis. Nat. Genet. 42, 72–76.

Bryant, D.M., and Mostov, K.E. (2008). From cells to organs: building polarized tissue. Nat. Rev. Mol. Cell Biol. 9, 887–901.

Chhabra, E.S., and Higgs, H.N. (2006). INF2 is a WASP homology 2 motif-containing formin that severs actin filaments and accelerates both polymerization and depolymerization. J. Biol. Chem. 281, 26754–26767.

Chhabra, E.S., Ramabhadran, V., Gerber, S.A., and Higgs, H.N. (2009). INF2 is an endoplasmic reticulum-associated formin protein. J. Cell Sci. 122, 1430–1440.

Cohen, D., Brennwald, P.J., Rodriguez-Boulan, E., and Müsch, A. (2004). Mammalian PAR-1 determines epithelial lumen polarity by organizing the microtubule cytoskeleton. J. Cell Biol. 164, 717–727.

de Marco, M.C., Martin-Belmonte, F., Kremer, L., Albar, J.P., Correas, I., Vaerman, J.P., Marazuela, M., Byrne, J.A., and Alonso, M.A. (2002). MAL2, a novel raft protein of the MAL family, is an essential component of the machinery for transcytosis in hepatoma HepG2 cells. J. Cell Biol. 159, 37–44.

de Marco, M.C., Puertollano, R., Martínez-Menárguez, J.A., and Alonso, M.A. (2006). Dynamics of MAL2 during glycosylphosphatidylinositol-anchored protein transcytotic transport to the apical surface of hepatoma HepG2 cells. Traffic 7, 61–73.

Faix, J., and Grosse, R. (2006). Staying in shape with formins. Dev. Cell 10, 693–706.

Fanayan, S., Shehata, M., Agterof, A.P., McGuckin, M.A., Alonso, M.A., and Byrne, J.A. (2009). Mucin 1 (MUC1) is a novel partner for MAL2 in breast carcinoma cells. BMC Cell Biol. 10, 7.

Fernandez-Borja, M., Janssen, L., Verwoerd, D., Hordijk, P., and Neefjes, J. (2005). RhoB regulates endosome transport by promoting actin assembly on endosomal membranes through Dia1. J. Cell Sci. 118, 2661–2670.

Gasman, S., Kalaidzidis, Y., and Zerial, M. (2003). RhoD regulates endosome dynamics through diaphanous-related formin and Src tyrosine kinase. Nat. Cell Biol. 5, 195–204.

Georgiou, M., Marinari, E., Burden, J., and Baum, B. (2008). Cdc42, Par6, and aPKC regulate Arp2/3-mediated endocytosis to control local adherens junction stability. Curr. Biol. 18, 1631–1638.

Goode, B.L., and Eck, M.J. (2007). Mechanism and function of formins in the control of actin assembly. Annu. Rev. Biochem. 76, 593–627.

Jaffe, A.B., Kaji, N., Durgan, J., and Hall, A. (2008). Cdc42 controls spindle orientation to position the apical surface during epithelial morphogenesis. J. Cell Biol. 183, 625–633.

Kovar, D.R., and Pollard, T.D. (2004). Insertional assembly of actin filament barbed ends in association with formins produces piconewton forces. Proc. Natl. Acad. Sci. USA 101, 14725–14730.

Kozlov, M.M., and Bershadsky, A.D. (2004). Processive capping by formin suggests a force-driven mechanism of actin polymerization. J. Cell Biol. 167, 1011–1017.

Maples, C.J., Ruiz, W.G., and Apodaca, G. (1997). Both microtubules and actin filaments are required for efficient postendocytotic traffic of the polymeric immunoglobulin receptor in polarized Madin-Darby canine kidney cells. J. Biol. Chem. *272*, 6741–6751.

Marazuela, M., Martin-Belmonte, F., Garcia-Lopez, M.A., Aranda, J.F., de Marco, M.C., and Alonso, M.A. (2004). Expression and distribution of MAL2, an essential element of the machinery for basolateral-to-apical transcytosis, in human thyroid epithelial cells. Endocrinology *145*, 1011–1016.

Martin-Belmonte, F., Gassama, A., Datta, A., Yu, W., Rescher, U., Gerke, V., and Mostov, K. (2007). PTEN-mediated apical segregation of phosphoinositides controls epithelial morphogenesis through Cdc42. Cell *128*, 383–397.

Massarwa, R., Schejter, E.D., and Shilo, B.-Z. (2009). Apical secretion in epithelial tubes of the *Drosophila* embryo is directed by the formin-family protein Diaphanous. Dev. Cell *16*, 877–888.

Mellman, I., and Nelson, W.J. (2008). Coordinated protein sorting, targeting and distribution in polarized cells. Nat. Rev. Mol. Cell Biol. *9*, 833–845.

Otomo, T., Otomo, C., Tomchick, D.R., Machius, M., and Rosen, M.K. (2005). Structural basis of Rho GTPase-mediated activation of the formin mDia1. Mol. Cell *18*, 273–281.

Ploubidou, A., and Way, M. (2001). Viral transport and the cytoskeleton. Curr. Opin. Cell Biol. *13*, 97–105.

Ridley, A.J. (2006). Rho GTPases and actin dynamics in membrane protrusions and vesicle trafficking. Trends Cell Biol. *16*, 522–529.

Rodriguez-Boulan, E., Kreitzer, G., and Musch, A. (2005). Organization of vesicular trafficking in epithelia. Nat. Rev. Mol. Cell Biol. *6*, 233–247.

Salvarezza, S.B., Deborde, S., Schreiner, R., Campagne, F., Kessels, M.M., Qualmann, B., Caceres, A., Kreitzer, G., and Rodriguez-Boulan, E. (2009). LIM kinase 1 and cofilin regulate actin filament population required for dynamin-dependent apical carrier fission from the *trans*-Golgi network. Mol. Biol. Cell *20*, 438–451.

Sormunen, R., Eskelinen, S., and Letho, V. (1993). Bile canaliculus formation in cultured HepG2 cells. Lab. Invest. *68*, 652–662.

Taunton, J. (2001). Actin filament nucleation by endosomes, lysosomes and secretory vesicles. Curr. Opin. Cell Biol. *13*, 85–91.

Wallar, B.J., DeWard, A.D., Resau, J.H., and Alberts, A.S. (2007). RhoB and the mammalian Diaphanous-related formin mDia2 in endosome trafficking. Exp. Cell Res. *313*, 560–571.

Wilson, S.H.D., Bailey, A.M., Nourse, C.R., Mattei, M.G., and Byrne, J.A. (2001). Identification of MAL2, a novel member of the MAL proteolipid family, through interactions with TPD52-like proteins in the yeast two-hybrid system. Genomics *76*, 81–88.

Xu, Y., Moseley, J.B., Sagot, I., Poy, F., Pellman, D., Goode, B.L., and Eck, M.J. (2004). Crystal structures of a formin homology-2 domain reveal a tethered dimer architecture. Cell *116*, 711–723.

Yang, C., Czech, L., Gerboth, S., Kojima, S.-i., Scita, G., and Svitkina, T. (2007). Novel roles of formin mDia2 in lamellipodia and filopodia formation in motile cells. PLoS Biol. *5*, e317.